Numerical and experimental validation of a hybrid finite element-statistical energy analysis method

Vincent Cotoni[a] and Phil Shorter
ESI US R&D, 12555 High Bluff Drive, Suite 250, San Diego, California

Robin Langley
Department of Engineering, University of Cambridge, Trumpington Street, Cambridge, CB2 1PZ, United Kingdom

(Received 22 August 2006; revised 12 April 2007; accepted 21 April 2007)

The finite element (FE) and statistical energy analysis (SEA) methods have, respectively, high and low frequency limitations and there is therefore a broad class of "mid-frequency" vibro-acoustic problems that are not suited to either FE or SEA. A hybrid method combining FE and SEA was recently presented for predicting the steady-state response of vibro-acoustic systems with uncertain properties. The subsystems with long wavelength behavior are modeled deterministically with FE, while the subsystems with short wavelength behavior are modeled statistically with SEA. The method yields the ensemble average response of the system where the uncertainty is confined in the SEA subsystems. This paper briefly summarizes the theory behind the method and presents a number of detailed numerical and experimental validation examples for structure-borne noise transmission. © *2007 Acoustical Society of America.* [DOI: 10.1121/1.2739420]

PACS number(s): 43.40.Qi, 43.40.Dx [LPF] Pages: 259–270

I. INTRODUCTION

The dynamic analysis of a complex vibro-acoustic system is difficult for two reasons: first the system may require many degrees of freedom to describe the response, and second the response may be sensitive to small imperfections in the system (arising, for example, from a given manufacturing process). Both of these problems become increasingly severe as the excitation frequency increases, due to the decreasing wavelength of the deformation. This situation is commonly encountered in the automotive industry, for example, where finite element (FE) models with several million degrees of freedom are often required to model the response of a vehicle to a few hundred hertz, while successive vehicles from a production line can show significant differences in their measured responses.[1,2]

When modeling the response of a vibro-acoustic system at higher frequencies it is therefore desirable to adopt an analysis method that provides statistical information and requires relatively few degrees of freedom. Statistical energy analysis (SEA)[3] provides such a method as a system is modeled as an assembly of relatively few subsystems, and the method gives the "mean" vibrational energy level in each subsystem (averaged across an ensemble of nominally identical systems). The approach is also capable of predicting the ensemble variance of the energy levels,[3,4] giving a measure of the statistical spread in the response. One of the assumptions in SEA is that the dynamic properties of the subsystems are very uncertain. If a subsystem is large compared with a deformation wavelength, then this assumption is typically valid and the "ensemble-average" response given by an SEA model provides a useful way to characterize the response of a system. However, at mid and low frequencies, this assumption may not be valid for all subsystems and the resulting ensemble average response becomes less useful.

This mix of dynamic behavior in which some subsystems are large compared with a wavelength (and are therefore well modeled by SEA), while others are short compared with a wavelength (and are not well modeled by SEA) is commonly encountered at mid frequencies. For example, consider the structure shown in Fig. 1, in which a number of thin panels are bolted to a stiff framework. Above 50 Hz, the wavelength of free flexural waves in the panels is much shorter than the panel dimensions; the bending modes of the panels are then typically very sensitive to perturbations. Conversely, the framework is very stiff and consequently exhibits few modes, which are insensitive to perturbation over a wide frequency range. In order to investigate the sensitivity of the response of the built-up structure, the panels were perturbed by adding a number of small masses at random locations, and a numerical Monte Carlo analysis was performed for different realizations of the mass positions. The structure was excited by a point force on the framework and the modulus squared velocity at a point on a panel was computed for each realization, as shown in Fig. 1. The results for 200 realizations are plotted in gray and one particular realization is plotted with a dotted line. The bold curve is the ensemble-averaged response. The response varies significantly from one realization to another, and the prediction of the response of one given configuration does not provide meaningful information regarding the behavior of the random ensemble. It is of more interest to consider the statistical properties of the response, such as the ensemble mean. The mean response exhibits distinct peaks that can be traced to the robust dynamic properties of the framework. Typically, a

[a]Author to whom correspondence should be addressed. Electronic mail: vincent.cotoni@esi-group-na.com

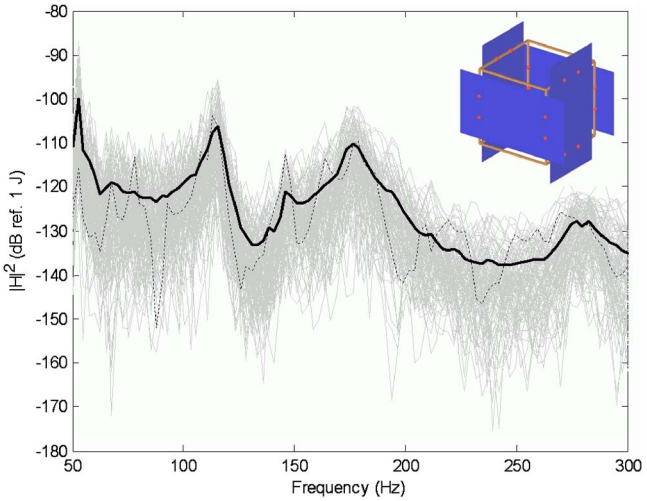

FIG. 1. (Color online) Typical modulus squared displacement response of an ensemble of slightly perturbed framework-panel structures at mid frequencies. Gray: a set of 200 Monte Carlo realizations; dotted: one particular Monte Carlo realization; thick black: ensemble average.

SEA model of the framework and panel would fail to describe this trend (since a SEA model implicitly assumes that the dynamic properties of the framework are very uncertain), while a FE model would be computationally expensive to apply to even a single realization of a more realistic structure. This example highlights the need for a hybrid modeling approach for describing the response of a system in the mid-frequency range.

The literature on mid-frequency analysis is extensive, and several authors have discussed attempts to combine deterministic and statistical analysis methods into a single model. The objective of a hybrid FE-SEA (or more generally deterministic-statistical) method is to combine the low frequency performance of the FE method with the high frequency performance of SEA to produce a robust technique that can be applied across a wide frequency range. However, the coupling of FE and SEA in a single model is difficult because the methods differ in two ways: (i) FE is based on dynamic equilibrium while SEA is based on the conservation of energy flow, and (ii) FE is a deterministic method while SEA is inherently statistical.

Belyaev and Palmov[5] included locally averaged statistical behavior into a global deterministic model of a system. This type of approach was developed further by Soize[6] in "fuzzy structure" theory. Langley and Bremner[7] developed a hybrid FE-SEA method based on these ideas combined with a wavelength partitioning scheme. Jayachandran and Bonilha[8] developed a hybrid technique where the structural vibration response obtained from SEA is used to excite a modal model of an interior acoustic space. Grice and Pinnington[9], Ji, Mace, and Pennington,[10] and Hong, Wang, and Vlahopoulos[11] also each developed hybrid methods in a series of papers (only the most recent references are given here) in which the short wavelength components are described statistically by effective impedances applied to the long wavelength components. The approaches differ in the way the effective impedance is computed and in the way the response of the short wavelength components is recovered. Most of those approaches assume that a statistical subsystem acts as an energy sink and therefore do not explicitly account for the flow of energy back into a deterministic subsystem. While such an assumption is often adequate for heavily damped subsystems (and/or weakly coupled subsystems), the assumption is not applicable for more general lightly damped reverberant systems.

Recently Shorter and Langley[12] developed a general method for coupling FE and SEA based on wave concepts rather than the modal-type of approach employed in Ref. 7. At the heart of the method is a reciprocity result[13,14] regarding the forces exerted at the boundaries of a SEA subsystem. The method yields the average response over an ensemble of random systems where the randomness is confined in the components described with SEA (recent work has also focused on the prediction of the variance of the response in the hybrid method, allowing prediction of the spread of the response around the mean value[15]).

The main aim of the present paper is to assess the performance of the hybrid FE-SEA method for predicting the ensemble average response of a number of example structures. The hybrid FE-SEA method is summarized in the following section, and numerical and experimental validation studies are reported in Sec. III.

II. HYBRID FE-SEA METHOD

A. Concept of "direct field" dynamic stiffness matrix

As discussed in the previous section, in the mid-frequency range some components of a complex structure (for example, thin panels) typically display short wavelength response and are sensitive to the effects of random uncertainties, while others (for example, stiff beams) show little variation in their dynamic properties and are essentially deterministic. In the hybrid method proposed by Shorter and Langley,[12] the deterministic components are modeled using the finite element method, while the random components are modeled as SEA subsystems. A key feature of the method is the concept of a direct field dynamic stiffness matrix associated with each SEA subsystem

Consider, for example, a thin plate that is excited at the boundaries. The excitation generates waves that propagate through the plate and are reflected repeatedly at the boundaries; the total dynamic stiffness matrix of the plate, phrased in terms of the edge degrees of freedom, has contributions from all of these reflections. Suppose now that the response is viewed in two parts: (i) the contribution from the initial generated waves, prior to any boundary reflections—this can be called the direct field; (ii) the contribution from waves produced on the first and all subsequent reflections—this can be called the "reverberant field." The direct field dynamic stiffness matrix can be defined as that resulting from the presence of the direct field waves. The presence of uncertainties in the system is accounted for in the reflections of the waves on boundaries and interior scattering devices, with the result that the direct field dynamic stiffness matrix is deterministic across the ensemble. Such a matrix can in principle

be computed from a boundary element analysis. However, in many instances, analytical approaches can be used to find the matrix.

Consider a thin plate bolted to a structural component at a point. The direct field dynamic stiffness of the plate as seen from the bolt can be obtained for any value of the bolt diameter by using recently developed analytical formulas.[16] These formulas are obtained by describing the displacement and stress fields at the bolt-plate interface in terms of a series of outgoing cylindrical waves (composed of Bessel functions), and by solving for the wave amplitudes using displacement compatibility and force equilibrium. In physical coordinates, this dynamic stiffness matrix is a 6×6 matrix relating the three displacements and three rotations at the connecting point to the three forces and three moments. If only the flexural wave field is considered in the description of the panel, the dynamic stiffness matrix reduces to a 3×3 matrix. If N bolts connect the plate with the structural component, then in principle the analysis should account for the coherence of the waves emanating from each bolt. The $6N\times6N$ direct field dynamic stiffness matrix would then be widely populated. However, if the wavelength of a free wave in the plate is short compared to the spacing between the bolts, then the phase of a wave arriving at a bolt is extremely sensitive to perturbation, and the resulting coherence can be neglected. In this case, the direct field dynamic stiffness can be derived from the analysis of each connection in isolation.

Consider now a thin plate connected to structural components, such as beams or frames, along the plate boundaries. If the plate is to be described by SEA and the structural components with FE, then the degrees of freedom of the boundary can be described in terms of the physical nodal degrees of freedom of the FE mesh. If the boundaries are straight, the direct field dynamic stiffness matrix associated with those degrees of freedom can be found by considering each straight boundary in turn, and taking it to form a segment of the edge of a semi-infinite plate. Motion of the boundary will generate waves into the semi-infinite plate, and for a given boundary motion the generated waves can be found by Fourier transform techniques, as detailed in the Appendix . The entries of the dynamic stiffness matrix are then found from the prescribed motion shapes and the boundary forces associated with the generated waves: i.e., strictly the dynamic stiffness matrix of a segment of the edge of a semi-infinite plate, when the motion of the segment is described by FE nodal degrees of freedom. This is the required direct field dynamic stiffness matrix for the plate edge, and by neglecting the coherence between the waves emanating from each plate edge, the process can be repeated for each of the edges to give the total direct field dynamic stiffness matrix of the plate subsystem. Another approach would be to model the vibration of the plate as a combination of incoming cylindrical waves (each carrying energy away from the boundary towards the center of the plate) and then use point collocation to assemble the direct field dynamic stiffness matrix for the boundary degrees of freedom.[17]

Given the concept of the direct field dynamic stiffness matrix, the hybrid FE-SEA equations can now be described.

B. Hybrid FE-SEA equations

The starting point for the hybrid method is to identify those parts of the system response that will be described by SEA subsystems. The remaining part of the system (which can be considered to be the "deterministic" part) is then modeled by using the FE method. The degrees of freedom associated with the SEA subsystems will be omitted from the FE model of the system, at all points other than the subsystems' boundaries. The relevant direct field dynamic stiffness matrix is then added to the FE model at the subsystems' boundaries, and this augmented FE model is used in the subsequent analysis. If the degrees of freedom of the FE part are labeled $\mathbf{q}$, then the governing equations of motion (for harmonic vibration of frequency ω say) will have the form

$$\mathbf{D}_{\text{tot}}\mathbf{q} = \mathbf{f} + \sum_k \mathbf{f}_{\text{rev}}^{(k)}, \tag{1}$$

$$\mathbf{D}_{\text{tot}} = \mathbf{D}_d + \sum_k \mathbf{D}_{\text{dir}}^{(k)}. \tag{2}$$

The summation is over the number of SEA subsystems in the model, and $\mathbf{D}_{\text{dir}}^{(k)}$ represents the direct field dynamic stiffness matrix associated with subsystem k at frequency ω. Furthermore, $\mathbf{D}_d$ is the dynamic stiffness matrix given by the finite element model of the deterministic part of the system (i.e., generally written in terms of a mass, stiffness and damping matrices, and the frequency), $\mathbf{f}$ is the set of external forces applied to this part of the system, and $\mathbf{f}_{\text{rev}}^{(k)}$ represents the force arising from the reverberant field in subsystem k (which is not accounted for in $\mathbf{D}_{\text{dir}}^{(k)}$ only including the direct field effect). The matrix $\mathbf{D}_{\text{tot}}$ is the dynamic stiffness matrix of the FE model (excluding the SEA subsystem degrees of freedom), when augmented by the direct field dynamic stiffness matrix of each SEA subsystem. It should be noted that Eqs. (1) and (2) are exact—all that has been done is to split the forces arising from the SEA subsystems into a direct field part, which is accounted for by $\mathbf{D}_{\text{dir}}^{(k)}$, and a reverberant part which is carried to the right hand side of Eq. (1). The following result[13,14] regarding the cross-spectral matrix of the reverberant blocked force is central to the development of the hybrid method:

$$\mathbf{S}_{ff,\text{rev}}^{(k)} \equiv \text{E}[\mathbf{f}_{\text{rev}}^{(k)}\mathbf{f}_{\text{rev}}^{(k)*\text{T}}] = \left(\frac{4E_k}{\omega\pi n_k}\right)\text{Im}\{\mathbf{D}_{\text{dir}}^{(k)}\}. \tag{3}$$

Here E[] denotes the ensemble average, where the ensemble describes a state of maximum uncertainty in the SEA subsystem with a given modal density, damping and direct field dynamic stiffness at the junction.[13] E_k and n_k are, respectively, the ensemble average energy and the modal density of the kth subsystem. Equation (3) implies that the cross-spectral matrix of the force exerted by the reverberant field on its surrounding boundaries is proportional to the resistive part of the direct field dynamic stiffness matrix of the boundary, and to the energy of the reverberant field. This forms a diffuse field reciprocity statement, and was shown to be valid when the (ensemble average) response of the subsystem constitutes a diffuse random wave field.[14] Equation (3) makes a connection between the energetics of the subsystem and the

elastic forces at the boundary, and as such it forms the key to coupling SEA to FE.

From Eq. (1), the response $\mathbf{q}$ can be expanded in the form

$$\mathbf{q} = \mathbf{q}_d + \sum_k \mathbf{q}^{(k)}, \quad \mathbf{q}_d = \mathbf{D}_{\text{tot}}^{-1}\mathbf{f}, \quad \mathbf{q}^{(k)} = \mathbf{D}_{\text{tot}}^{-1}\mathbf{f}_{\text{rev}}^{(k)}. \tag{4}$$

Now the ensemble and time averaged power input to the direct field of subsystem j can be written as

$$P_{\text{in},j} = (\omega/2)\text{Im}\{\text{E}[\mathbf{q}^{*\text{T}}\mathbf{D}_{\text{dir}}^{(j)}\mathbf{q}]\} = (\omega/2)\sum_{rs} \text{Im}\{D_{\text{dir},\text{rs}}^{(j)}\}S_{qq,rs}, \tag{5}$$

where it has been noted that the direct field dynamic stiffness matrix is symmetric and is fixed across the ensemble. Due to the statistical nature of the reverberant response of the subsystems, the various contributions $\mathbf{q}^{(k)}$ that appear in Eq. (4) are taken to be uncorrelated and of zero mean, and Eqs. (3)–(5) then yield

$$P_{\text{in},j} = P_{\text{in},j}^{\text{ext}} + \sum_k \omega\eta_{jk}n_j(E_k/n_k), \tag{6}$$

where

$$P_{\text{in},j}^{\text{ext}} = (\omega/2)\sum_{rs} \text{Im}\{D_{\text{dir},rs}^{(j)}\}(\mathbf{D}_{\text{tot}}^{-1}\mathbf{S}_{ff}\mathbf{D}_{\text{tot}}^{-1*\text{T}})_{rs}, \tag{7}$$

$$\omega\eta_{jk}n_j = (2/\pi)\sum_{rs} \text{Im}\{D_{\text{dir},rs}^{(j)}\}(\mathbf{D}_{\text{tot}}^{-1}\,\text{Im}\{\mathbf{D}_{\text{dir}}^{(k)}\}\mathbf{D}_{\text{tot}}^{-1*\text{T}})_{rs}. \tag{8}$$

In Eq. (7), $\mathbf{S}_{ff}$ denotes the cross-spectral matrix of the external forces applied to the FE part. Given that the dynamic stiffness matrices are symmetric, it is readily shown from Eq. (8) that reciprocity holds, in the sense that $\eta_{jk}n_j = \eta_{kj}n_k$. As will be shown in what follows, the terms η_{jk} are equivalent to the coupling loss factors that appear in SEA.

The ensemble averaged power output from the reverberant field in subsystem j can be written as the sum of the power dissipated through damping and the power output at the boundary

$$\begin{aligned} P_{\text{out},j} &= \omega\eta_j E_j + (\omega/2)\text{Im}\{\text{E}[\mathbf{q}^{(j)*\text{T}}\mathbf{f}_{\text{rev}}^{(j)}]\} \\ &= \omega\eta_j E_j + \sum_k \omega\eta_{kj}n_k(E_j/n_j) + \omega\eta_{d,j}E_j, \end{aligned} \tag{9}$$

where Eqs. (1)–(4) were used to express the expectation in terms of the subsystem energy and the various dynamic stiffness matrices. The last term in Eq. (9) is the power dissipated in the deterministic part of the system, given by

$$\omega\eta_{d,j} = \left(\frac{2}{\pi n_j}\right)\sum_{rs} \text{Im}\{D_{d,rs}\}(\mathbf{D}_{\text{tot}}^{-1}\,\text{Im}\{\mathbf{D}_{\text{dir}}^{(j)}\}\mathbf{D}_{\text{tot}}^{-1*\text{T}})_{rs}. \tag{10}$$

Equations (6) and (9) then lead to the following energy balance equation for subsystem j:

$$\omega(\eta_j + \eta_{d,j})E_j + \sum_k \omega\eta_{jk}n_j(E_j/n_j - E_k/n_k) = P_{\text{in},j}^{\text{ext}}. \tag{11}$$

Furthermore, the cross-spectral matrix of the response $\mathbf{q}$ can be derived from Eqs. (3) and (4), which yields

$$\mathbf{S}_{qq} = \mathbf{D}_{\text{tot}}^{-1}\left[\mathbf{S}_{ff} + \sum_k \left(\frac{4E_k}{\omega\pi n_k}\right)\text{Im}\{\mathbf{D}_{\text{dir}}^{(k)}\}\right]\mathbf{D}_{\text{tot}}^{-1*\text{T}}. \tag{12}$$

Equations (11) and (12) form the two main equations of the hybrid method. These equations couple FE and SEA methodologies: Eq. (11) has precisely the form of SEA, but the coupling loss factors η_{jk} and loss factors $\eta_{d,j}$ are calculated by using the FE model (augmented by the direct field dynamic stiffness matrices) via Eqs. (8) and (10); furthermore, Eq. (12) has the form of a standard random FE analysis, but additional forces arise from the reverberant energies in the SEA subsystems. If no SEA subsystems are included then the method becomes purely FE; on the other hand, if only the junctions between the SEA subsystems are modeled by FE, then the method becomes purely SEA, with a novel method of computing the coupling loss factors through complex and possibly dissipative junctions.

C. Steps in the Hybrid FE-SEA method

The first step when building a hybrid model of a system is to partition the system into deterministic and statistical portions. This partitioning can be based on the expected wavelengths within the various components of a system. The local dynamic response of a subsystem that is large compared to a wavelength is typically sensitive to perturbations, and an SEA description should be used; conversely, subsystems that are small compared with wavelength should be described with FE. Although the value defining small *versus* large wavelength depends on the actual level of uncertainty or perturbation (i.e., the dynamic properties of any components could eventually be made random by sufficiently increasing the level of the perturbations), the practical limit value of a few wavelengths within the component is typically used. It should be noted that the choice of partitioning implicitly defines the statistical ensemble in a hybrid analysis.

Once the partition is defined, the hybrid method proceeds as follows:

(1) A finite element model of the deterministic part of the system is constructed. All degrees of freedom associated with SEA subsystems are omitted from this model, other than those that lie on the subsystem boundaries.
(2) A direct field dynamic stiffness matrix is constructed for each SEA subsystem in terms of the relevant boundary degrees of freedom. These matrices are then coupled to the FE model to yield the total dynamic stiffness matrix $\mathbf{D}_{\text{tot}}$.
(3) The various terms that appear in the SEA equation, Eq. (11), are calculated from Eqs. (7), (8), and (10).
(4) The SEA equations are solved to yield the subsystem energies E_j.
(5) Given the SEA subsystem energies, Eq. (12) is used to yield the response of the deterministic part of the system.

A key feature of the method is that the FE mesh considered in step (1) does not need to capture the short wavelength response of the subsystems, and thus relatively few degrees of freedom are required compared to a conventional finite element model. This leads to very significant reductions in

the computer time and memory needed to solve the problem. Furthermore, the method immediately yields ensemble average response quantities, without any need for a Monte Carlo simulation of the ensemble.

III. EXAMPLE APPLICATIONS

Three validation studies are presented in this section. The first two are concerned with FE and SEA subsystems which are connected at discrete points, while the third involves extended connections along line junctions. In all cases, benchmark Monte Carlo results for the response of an ensemble of randomized structures have been obtained for comparison with the ensemble-averaged response yielded by the hybrid method. In the second case, the benchmark Monte Carlo results were obtained experimentally; in the other cases, the benchmark results were obtained from extensive detailed FE calculations.

The systems were randomized by attaching point masses at random locations on various components. Ten masses per component were considered, with a constant total added mass of 15% or 20% of the mass of the bare component depending on the particular example. When there is sufficient uncertainty in the dynamic properties of a system, the overall response statistics become insensitive to the way in which a system is randomized.[4,18] The use of point masses in the following examples is therefore representative of more general ensembles.

The predictions of the modulus squared velocity response at a number of locations on the structures are compared. For the hybrid results, if the point was located on the FE part, the modulus square velocity associated with the ith degree of freedom was obtained from Eq. (12) with $\mathrm{E}[|v_i|^2] = \omega^2\{S_{qq}\}_{ii}$. If the point belonged to an SEA subsystem, the response was recovered using the formula[3] $\mathrm{E}[|v_{i\in \mathrm{sub}k}|^2] = 2E_k/M_k$, where M_k is the mass of the subsystem and the energy is computed from Eq. (11).

A. Framework-panel structure: A numerical benchmark

1. Description of the structure

The hybrid method has been applied to the example structure shown in Fig. 1. The structure consists of a beam framework with four thin panels which are each bolted to the framework at four points. All components are made of aluminium with elastic properties $E=71$ GPa, $\nu=0.33$, and $\rho = 2700\ \mathrm{kg/m^3}$. The beams are all 0.7 m long, with a square hollow section of external side width 25.4 mm and wall thickness 3.2 mm. They are connected at right angles and form the edges of a cube. The panel dimensions are 0.6 m $\times$ 1.1 m, with thickness 1 mm. They are connected to the framework at four points with plain cylindrical bolts of 5 mm radius, with an offset of 17 mm to the neutral axis of the beams. Two successive bolts on a common beam are 0.2 m apart. The damping loss factor is 0.05% for the framework, and 2% for the panels.

Two excitation locations were considered: a point force was applied in the transverse direction on panel 1, or on one of the lower horizontal beams of the framework in the vertical direction at 0.25 m from the corner, as indicated by the arrow in the left hand picture of Fig. 2. Regarding the loading of the randomized panel, "rain-on-the-roof" excitation commonly used in SEA would yield the same ensemble mean response as the point force (but the variance of the response would be smaller).[4] The dynamic response was investigated at a point in each panel in the out-of-plane direction, and at two points on the framework. The observation point 1 on the framework is the same as the loading point and the same vertical direction is considered. The second point is on the other side of the framework at 0.25 m from the corner, and the horizontal direction is considered as shown on the left hand side of Fig. 2.

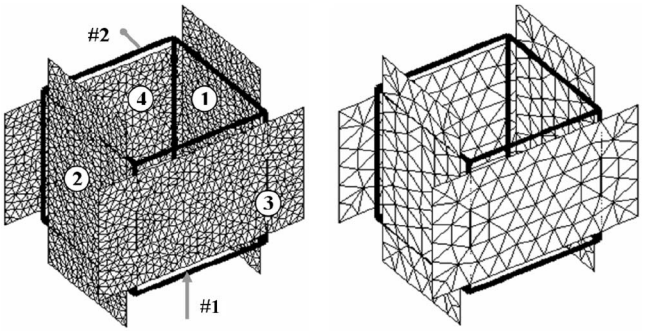

FIG. 2. Two finite element meshes of a framework-panel structure. Left: mesh for reference Monte Carlo simulation (10 481 degrees of freedom); right: mesh for hybrid prediction where the surface elements are membrane only (1184 degrees of freedom).

The reference results were obtained using the detailed FE model of the structure shown on the left hand side of Fig. 2. The FE software package VA ONE[19] was used to create the model composed of 10 481 degrees of freedom for analysis up to 300 Hz. The framework and bolts were described with 96 beam elements and the panels with 3354 triangular shell elements. The structure was randomized by adding a set of ten masses at random locations on each panel, each mass having 2% of the mass of the bare panel. By moving the masses to random locations, 200 realizations were generated for the Monte Carlo analysis.

2. Hybrid FE-SEA model

The partition of the system into deterministic and statistical subsystems can be based on the free propagating wavelengths across the frequency range of interest. The shear and extensional wavelengths in the panels are, respectively, 18 and 16 m at 300 Hz, suggesting that the in-plane motion associated with these waves should be described with FE. The bending wavelength in the panels is 0.31 m at 100 Hz, and 0.18 m at 300 Hz. This corresponds to between 2 and 4 wavelengths within the shortest dimension of the panels, which implies that the out-of-plane motion should be described with SEA. Below 50 Hz, this SEA description is not expected to be appropriate as the bending wavelength is larger than the panel dimensions, and strictly a FE description should be used. The first four propagating waves in the beams are a torsional wave, an extensional wave, and two bending waves (additional higher order wave types cut on

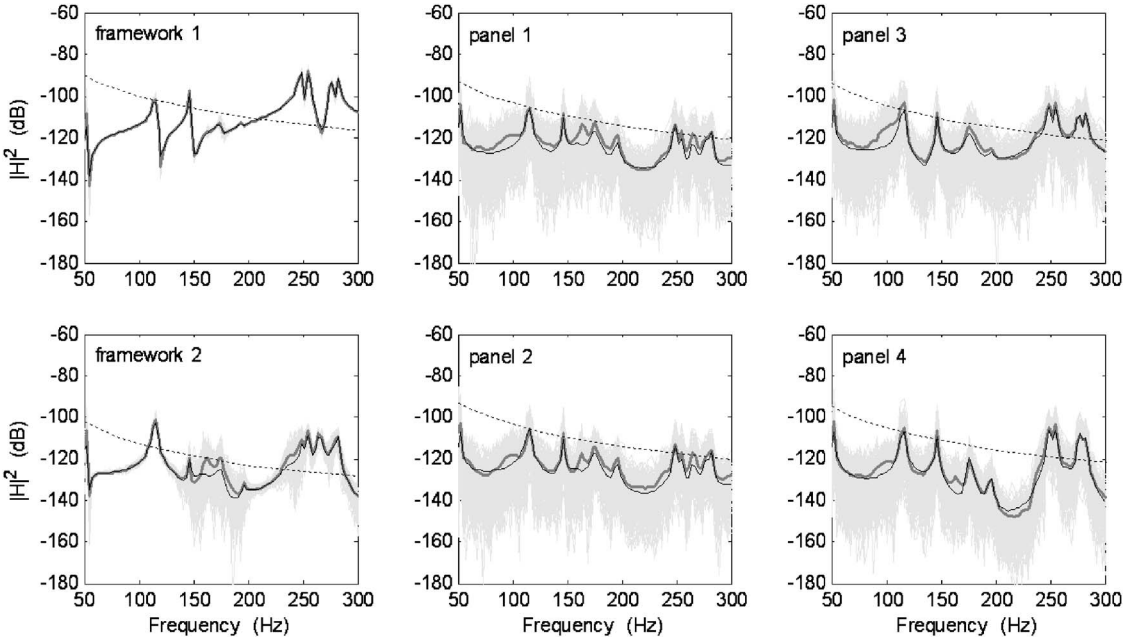

FIG. 3. Modulus squared velocity response of the framework-panel structure to a point force excitation applied on the framework. Light gray: each Monte Carlo realization; bold gray: Monte Carlo ensemble average. Solid black: hybrid FE-SEA; dotted: pure SEA.

above 9650 Hz). The corresponding wavelengths at 300 Hz are all larger than 1 m so that a FE description should be adopted for the beams.

There are approximately 250 bending modes in the four panels, no in-plane modes and approximately 30 modes in the framework. This emphasizes the efficiency gains that can be achieved by using a statistical description of the panel bending motion, rather than a detailed FE description.

The FE model employed in the hybrid method is shown on the right hand side of Fig. 2, and comprises 1184 degrees of freedom. The framework and bolts were described with the same elements and mesh as the reference Monte Carlo FE model. Conversely, the panels were described with a much coarser mesh composed of 520 triangular membrane elements, as only the in-plane motion is of concern. The coupling between the FE and SEA subsystems was described by a series of 16 point junctions. The various point junctions were assumed to be incoherent and the local direct field dynamic stiffness matrices were computed separately.

3. Comparison with Monte Carlo results

The velocity squared frequency response at two points of the framework and at one point of each panel is shown in Figs. 3 and 4 for excitation respectively on the framework, and on panel 1. The response for each Monte Carlo realization is plotted with a light gray line, the ensemble-averaged reference response with a bold gray line, and the hybrid FE-SEA prediction with a black line. In addition to the reference and hybrid results, the results from a pure SEA model (created using the software VA ONE[19]) are shown with dotted lines. In the SEA model, all the components are described with SEA: each of the 12 beams of the framework is described with four wave fields corresponding to the first four propagating waves (one extensional, two flexural, one torsional); each of the four panels is described with three wave fields (one extensional, one flexural, one shear). The complete SEA model is made of 60 SEA subsystems, all coupled through point junctions.

The hybrid prediction provides a good estimate of the ensemble average response, and significantly improves the SEA prediction. In particular, the hybrid approach is able to capture the "modal" behavior of the ensemble mean response arising from the robust dynamics of the framework. The overestimation of the response of the panels in the pure SEA model is due to the strong coupling provided by the long-wavelength subsystems (the framework and the in-plane motion of the plates). This can also be viewed as being due to a lack of a sufficient amount of uncertainty in the modal properties for these subsystems to be represented by SEA subsystems. Some differences between the reference results and the hybrid method are to be expected due to the limited number of trials used in the Monte Carlo simulation, and the lack of randomness introduced by the added masses (especially at lower frequencies).

It is noted in passing that the variance of the response depends on the load case, the observation location and the frequency; recent work has been directed at including variance prediction within the hybrid method.[15]

B. Framework-panel structure: An experimental benchmark

1. Structure and experimental setup

The hybrid method has been used to predict the response of the test structure shown in Fig. 5. The upper part of the structure is similar to the previous numerical example and consists of a cubic beam framework with four thin panels each bolted to the framework at four points. A number of viscoelastic patches are glued onto the thin panels in order to increase the damping, as shown in Fig. 5(b). Four additional circular hollow beams connect the cubic framework to a stiff

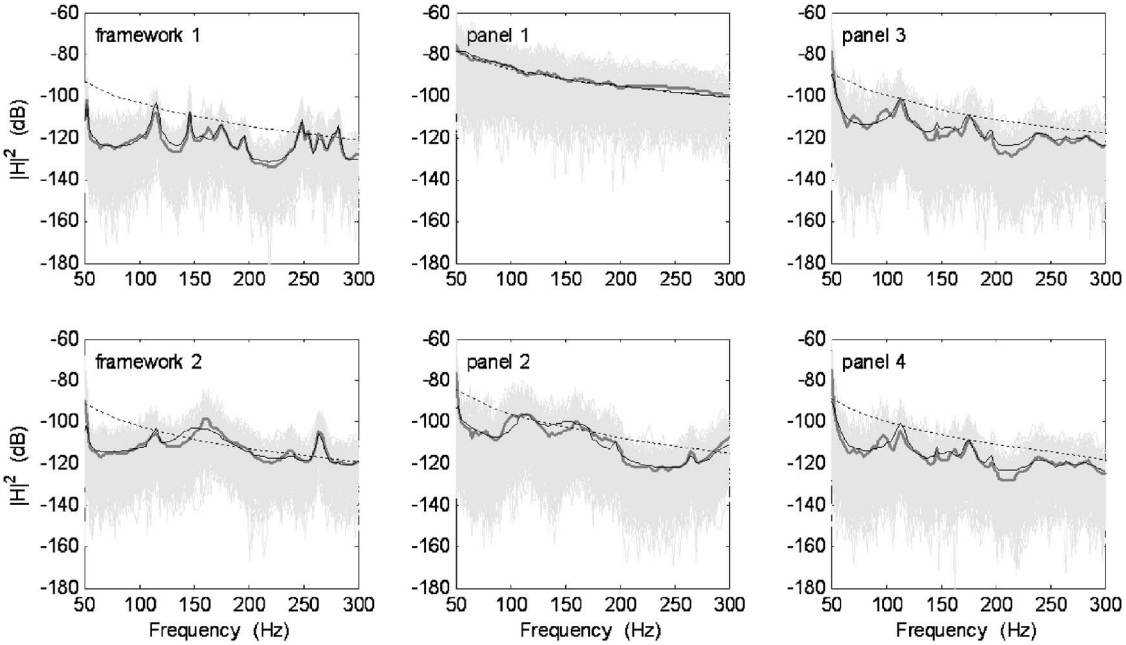

FIG. 4. Modulus squared velocity response of the framework-panel structure to a point force excitation applied on panel 1. Light gray: each Monte Carlo realization; bold gray: Monte Carlo ensemble average. Solid black: hybrid FE-SEA; dotted: pure SEA.

panel via welded junctions (see Fig. 5(a) where the thin panels are removed). The bottom panel is 6.35 mm thick and of dimensions 0.4 m × 0.4 m. The circular hollow beams are 1.3 m long and the section external diameter is 19 mm with wall thickness 1.6 mm. All components are made of aluminium.

The structure was randomized by attaching ten masses to each of the four thin panels at random locations (some masses can be seen in Fig. 5(b)), representing 18% of the mass of the bare panel. Twenty realizations of the structure were tested. The structure was suspended from a corner of the framework with an elastic string so that a close approximation to free boundary conditions was obtained. The framework was excited by an inertial shaker at the location referenced Acc 1 in Fig. 5(a), in the direction of the main axis of the structure (almost vertical in the picture). The shaker is shown in Fig. 5(b), and the precise location was 0.314 m from the closest framework corner. The acceleration response was measured on the framework at the two points Acc 1 and 2 indicated on Fig. 5(a), in the direction of the main axis. The second accelerometer was at 76.7 mm from the center of the bottom plate. The acceleration response was also measured at one point on each of the four panels in the out-of-plane direction. The points were chosen to be remote from the connection points and from the edges to avoid near-field and correlation effects. A white noise signal was applied to the shaker, and acceleration and input force data were measured up to 1000 Hz. The modulus square velocity responses per unit force were computed from the measured acceleration-force cross-spectra S_{af}, and the force auto-spectrum S_{ff}, by using the relation $|v(\omega)|^2 = |S_{af}(\omega)/S_{ff}(\omega)|^2/\omega^2$. The responses were then averaged over all realizations.

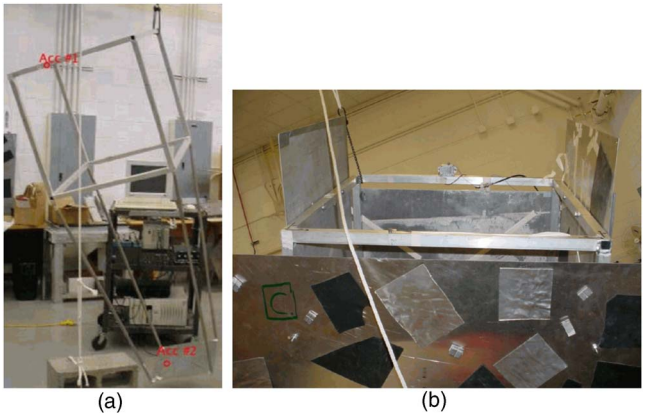

FIG. 5. (Color online) Test structure suspended from a corner. Left: framework and bottom thick plate alone; right: top part of the framework, with the four thin panels each bolted at four points. The inertial shaker used for excitation is on the more remote beam.

2. Hybrid FE-SEA model

The same approach as in the previous example was employed to build the hybrid model of the test structure: For a specified frequency range, the free wavelength of each component was compared to the characteristic dimension of the component in order to choose either an FE or an SEA description. The hybrid model of the structure was developed for analysis up to 1000 Hz. The bending wavelength of the thin panels becomes shorter than the panel dimension at about 30 Hz, and thus an SEA model was adopted. Conversely, the framework, the top plate and the in-plane motion of the panels were modeled by FE. The coupling between the FE model and the four SEA subsystems was achieved by a series of 16 point junctions using the direct field dynamic stiffness matrix from each connection in isolation.

The FE part of the hybrid model excluding the in-plane motion of the thin panels was first validated against experimental data obtained with the structure prior to the attach-

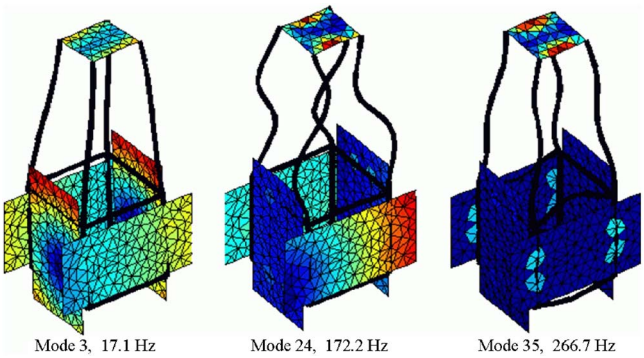

FIG. 6. (Color online) Selected mode shapes of the FE part of the hybrid model of the test structure. Only the membrane behavior of the four large panels is considered (bending is removed).

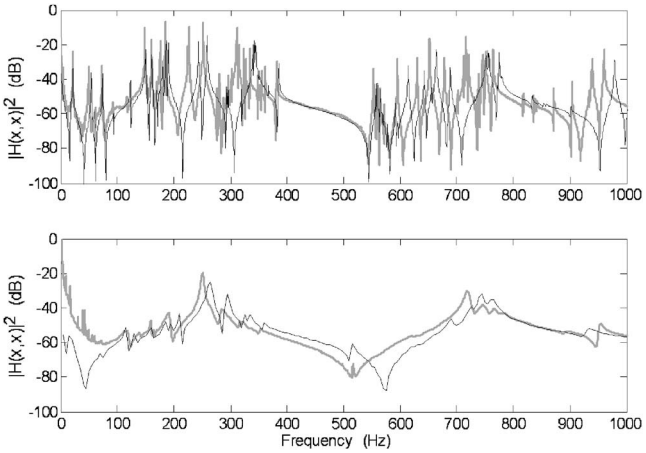

FIG. 7. Experimental (gray) and simulated (black) drive point mobility response of the test structure. Upper diagram: framework without panels (prediction by FE); lower diagram: framework with panels (prediction by hybrid FE-SEA).

ment of the thin panels (see Fig. 5(a)). The model was meshed with triangular shell elements for the top plate and beam elements for the framework, with a total of 876 degrees of freedom for analysis up to 1000 Hz. Starting with standard material properties for the aluminum ($E=71$ GPa, $\nu=0.33$, $\rho=2700$ kg/m^3), the model was updated by adding mass at the welded junctions, then adjusting the aluminum density to fit the mass of the test structure, and finally adjusting the Young modulus to fit the first few natural frequencies. A damping loss factor of 0.5% was found to give satisfactory predictions over the whole frequency range. The predicted and measured dynamic response of the structure at the drive point (point Acc 1 in Fig. 5(a)) are respectively shown with the black and gray lines on the top diagram of Fig. 7. The agreement is acceptable for the purposes of the study. It may seem that the experimental curve has more modes than the predicted one. The symmetry of the simulated structure might explain this: although lumped masses have been added in the model to account for the sensors and actuators, the perturbation may be too weak to break the symmetry and make all the modes appear in the predicted response. For example, between 300 and 400 Hz where five modes can be seen on the predicted response, closer examination shows that there actually are nine resonances. It is expected that with this level of accuracy for the base FE part of the model, the hybrid model will be accurate up to approximately 800 Hz.

The FE component of the complete hybrid model includes the in-plane motion of the panels. The resulting model comprises 68 shell elements (bottom plate), 1068 membrane elements (for the in-plane motion of the thin panels), and 204 beam elements (framework and bolts), giving a total of 924 nodes and 2659 degrees of freedom. The corresponding mesh is shown in Fig. 6. The bolts were described by using small beam elements with attention paid to the offset from the framework (which plays a significant role in the transmission of power to the flexural field of the panels).

A modal analysis was performed on the FE component of the hybrid model and 120 modes were extracted with frequencies below 1000 Hz. This is to be compared with more than 1000 modes that would arise if the bending modes of the panels were included. Some of the mode shapes are illustrated in Fig. 6. In most instances, the thin panels behave almost like rigid bodies (recall that only the in-plane motion is considered). Indeed, from a free wavelength analysis, it is found that the first membrane mode of the panels is expected to occur at around 2000 Hz. At lower frequencies the panels act to provide additional mass and static stiffness to the framework. Global modes of the type shown in Fig. 6 are expected to govern the ensemble-averaged response of the structure.

The bending motion of each panel was described with an SEA subsystem. The effect of the randomly added masses was distributed over the subsystem by increasing the mass density by a factor of 1.18. The damping of the panels was measured using the power injection method[3] with an instrumented hammer impact on a panel in isolation. The power input to the panel was estimated from the acceleration and force measurements at the impact point, and the energy was estimated from four accelerometers placed at random locations on the panel. The value of the damping loss factor calculated from a power balance at each frequency was found to be approximately constant across the frequency range of interest and equal to 1.1%.

3. Comparison with Monte Carlo experiment

The response of the structure due to a point force acting at the point Acc 1 in Fig. 5(a) was computed for each of the six observation points described above. The measured and computed drive point velocities are shown in the lower diagram of Fig. 7. For comparison, the measured and computed responses of the structure without the thin panels (see previous section) are shown in the upper diagram with the same vertical scale. The hybrid model reproduces some of the changes that occur when adding the thin panels to the framework. As already discussed, the membrane effect of the panel is mainly a reactive effect and this explains the shift of the natural frequencies. Conversely, the bending point impedance of the panels is resistive and corresponds mainly to a damping effect that changes the width of the resonance peaks (as seen in Fig. 7).

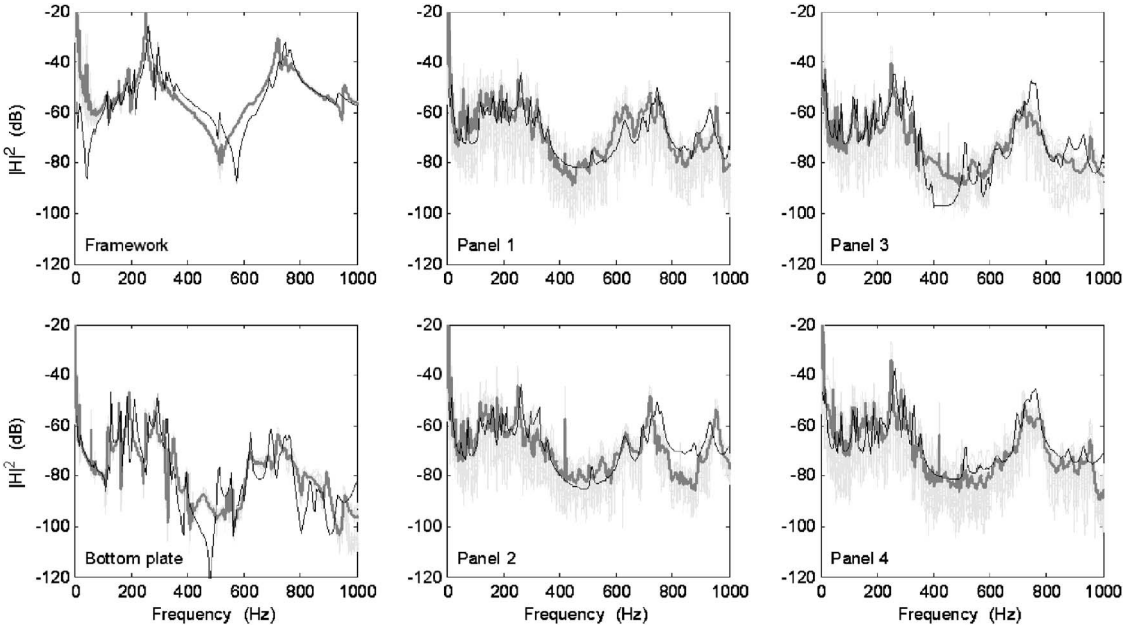

FIG. 8. Modulus squared velocity response at six locations of the test structure to a point force excitation on the framework. Light gray; 20 experimental realizations; bold gray: averaged experimental response; black: hybrid FE-SEA prediction.

The velocity squared response at each of the six observation points on the structure is shown in Fig. 8. Three sets of results are shown in each diagram: the experimental results for 20 realizations are shown in light gray; the ensemble-averaged experimental response is plotted with a bold gray line; and the hybrid prediction is plotted with a black line. The test data exhibit the mid-frequency characteristics, with a significant sensitivity of the response to perturbations, and at the same time some distinct features (peaks and drops) in the ensemble mean response. Those features are reasonably well predicted by the hybrid method. For instance, the response maximum at 260 Hz can be traced to global mode 35 (266 Hz) in Fig. 6; this mode has a large displacement at the excitation location in the direction of the excitation, and consequently features strongly in the hybrid prediction. It also appears in the experimental averaged data although it is not an actual natural mode of vibration of any single realization of the ensemble. The prediction, however, is not perfect. As previously noted, the FE model of the framework is valid only up to 800 Hz, and this might explain the approximate results yielded by the hybrid method above that frequency. This emphasizes the need for an accurate description of the deterministic part of the hybrid model: as the system randomness is assumed to arise in the short-wavelength components, only those components are suitable to a coarse description as provided by SEA. Any errors in the FE model will clearly propagate through to the response prediction.

The first two test cases above demonstrated how statistics can be included in a traditional FE model using the hybrid method. It is noticed that no explicit information was specified regarding the nature of the uncertainty of the SEA subsystems. It has been shown that the statistics underlying the SEA diffuse reverberant field concept corresponds to a state of maximum uncertainty,[13] and as such may not be identical to the actual uncertainty in a given structure. However, in most practical cases of engineering interest, very little is known about the actual uncertainty, and a state of maximum uncertainty provides a pragmatic approach that can be readily included in a model. In addition, recent studies have shown that the dynamic properties of an uncertain system at high frequencies exhibit the same universal statistics regardless of the exact nature of the uncertainty provided that the system is random enough.[4,18] It is then expected that the hybrid method yields an appropriate prediction of the ensemble average response of a system provided the subsystems modeled with SEA exhibit a sufficient amount of randomness across the actual ensemble.

C. Two panels connected by an extended line junction

Consider the structure shown in Fig. 9; two identical

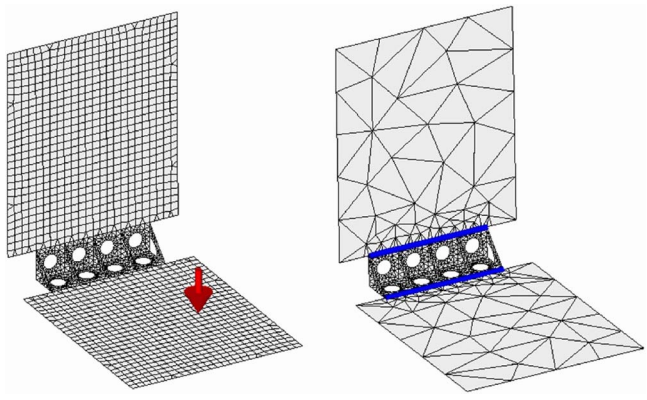

FIG. 9. (Color online) Two finite element meshes of a bracket-panels structure. Left: detailed mesh for Monte Carlo simulation (11 922 degrees of freedom); Right: mesh for hybrid prediction where the surface elements are membrane only (3502 degrees of freedom). The bold lines are the hybrid line junctions between the finite element freedoms and the panels bending wave fields described by SEA.

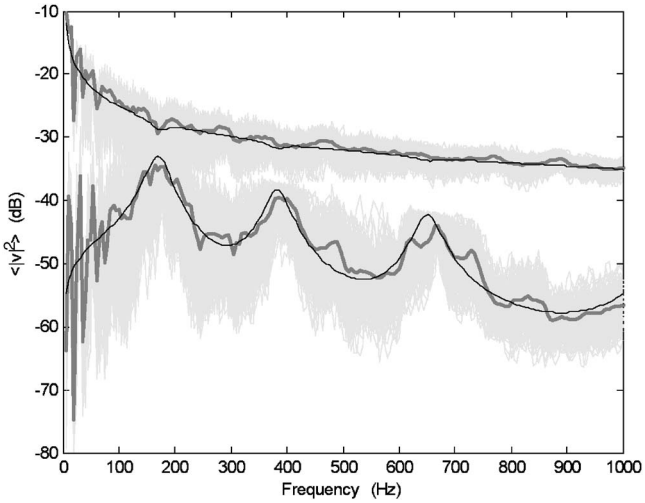

FIG. 10. Mean squared velocity response in the source and receiving plates. Light gray: reference Monte Carlo results for 200 realizations; bold gray: Monte Carlo ensemble average; black: hybrid FE-SEA.

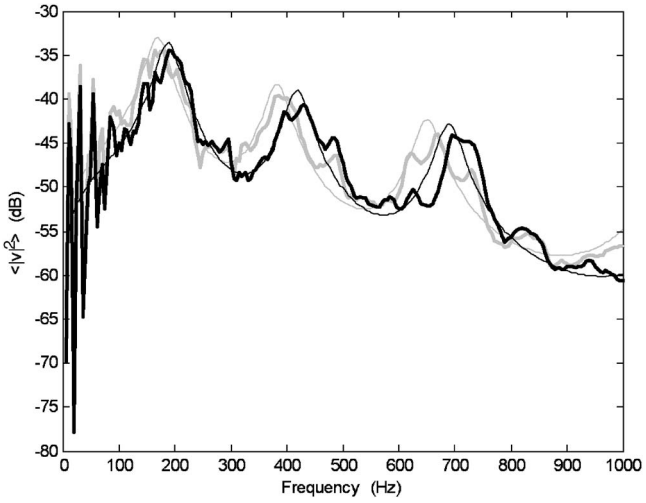

FIG. 11. Mean squared velocity response in the receiving plate for pinned (gray) and clamped (black) nodes at the bracket ends. Bold: Monte Carlo ensemble average; thin: hybrid FE-SEA.

thin aluminum plates of dimension 0.6 m $\times$ 0.7 m and thickness 1 mm are coupled by a stiff bracket. Interest lies in predicting the transmission of structure-borne noise between the two plates when one plate is excited by spatially distributed (rain-on-the-roof) excitation. The bracket is 0.4 m long and is made of 4 mm thick steel. The three corner points at each end of the bracket are pinned. The structure has a uniform damping loss factor of 1%.

A reference FE model with triangular and quadrangular shell elements was created with 551 nodes in the bracket and 773 nodes per panel; 370 modes were extracted with frequencies below 1200 Hz. In order to reduce computational expense when performing a Monte Carlo simulation, a component mode synthesis model was created using three super elements, and the space-averaged squared velocity in the plates due to rain-on-the-roof excitation was then calculated using the energy flow postprocessing equations presented by Mace and Shorter.[20] A Monte Carlo simulation was performed by adding ten masses to each plate at random locations, each mass being 0.5% of the total mass of the structure. The velocity response computed using the FE Monte Carlo simulation is plotted in Fig. 10. The transmission across the bracket is clearly sensitive to perturbation, while the ensemble average transmission exhibits a number of distinct peaks that are related to the local dynamic behavior of the bracket (the relative variance of the response in the receiving plate is significantly reduced around these peaks).

A hybrid model was created in which the stiff bracket was modeled in detail with FE using the same shell elements, and the (long wavelength) membrane behavior of the plates was modeled using a coarse mesh of triangular membrane elements (74 nodes per plate). The (short wavelength) flexural wave fields of the plates were modeled using two SEA subsystems. Two hybrid line junctions were used to couple the FE and SEA subsystems together. The hybrid line junction formulation described in the Appendix provides a method for calculating the direct field dynamic stiffness of an SEA subsystem. A modal analysis was performed on the FE subsystem and six modes were retained below 1200 Hz (to be compared with the 370 modes of the full FE model). Two of those modes at 547 and 554 Hz only involve the in-plane motion of the panels, and they are not expected to affect the response. The other modes at, respectively, 196, 428, 701, and 1200 Hz involve torsion of the bracket with simply supported ends. A point force was applied to one of the SEA subsystems and the hybrid model was used to calculate the response. The solution is computationally efficient and took approximately 1/100th of the time it took to compute 20 Monte Carlo trials. The ensemble average response predicted with the hybrid FE-SEA approach is in good agreement with the FE Monte Carlo simulations. In particular, the peak in the transmission can be explained by the local modal dynamics of the brackets (modified by the reactive and resistive impedance of the direct fields of the panels). The reactive part can be seen to be mainly a mass effect since the peaks in the transmission are lower in frequency than the natural frequencies of the bracket in isolation.

The computational efficiency of the hybrid approach enables robust design changes (i.e., design changes that are insensitive to uncertainties) to be quickly identified. As an example, the following section investigates modifications to the boundary conditions of the bracket and the value of damping. The resulting hybrid predictions are compared with additional FE Monte Carlo computations.

In the initial configuration, three nodes at each end of the bracket were pinned. This boundary condition was changed to clamped nodes and the hybrid model was re-run using the updated modes for the FE portion of the structure. The ensemble averaged mean squared velocity response of the transmitted plate obtained by the hybrid and Monte Carlo simulations is shown in Fig. 11. The initial configuration results from Fig. 10 are plotted in gray. The Monte Carlo results show that the primary effect of changing the bracket boundary conditions is to increase the frequency of the peaks in the transmission (arising from the stiffening of the structure). This change is correctly predicted by the hybrid model.

Keeping the initial boundary conditions, the damping loss factor of the bracket was changed from 1 to 10%. The

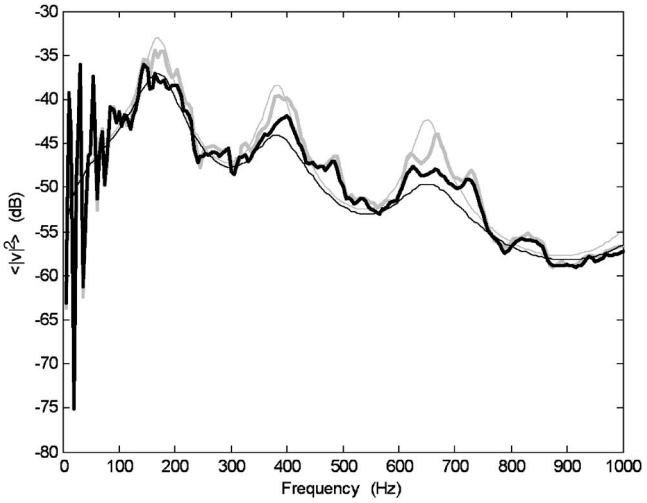

FIG. 12. Mean squared velocity response in the receiving plate for two values of damping loss factor of the bracket: 1% (gray) and 10% (black). Bold: Monte Carlo ensemble average; thin: hybrid FE-SEA.

ensemble averaged mean squared velocity response of the transmitted plate is shown in Fig. 12, where good agreement is seen between the Monte Carlo and hybrid results.

This last test case is typical of a problem traditionally handled by SEA, as interest lies in predicting the energy transmission between two subsystems with high modal density. The example shows how the hybrid method can be used to enhance a pure SEA model by providing a rigorous and automatic calculation of the SEA coupling loss factors. The method enables an arbitrary amount of deterministic detail to be added to a junction (for example, detailed modifications to the boundary conditions of the junction), and allows the junction to be dissipative (which is often problematic in traditional SEA). Similarly, by describing the vicinity of some external excitations with FE while keeping the rest of the model with SEA, the hybrid method can be used to improve the estimation of the power input into an SEA model. This application is not demonstrated here.

IV. CONCLUSIONS

A hybrid analysis method has been discussed which combines the finite element method with statistical energy analysis. The combination of these two methods in the same model provides an efficient way to model the vibro-acoustic behavior of systems with mid-frequency behavior. In particular, (i) components with few modes (or long wavelength behavior) are described deterministically with FE, as their dynamic behavior is robust to uncertainty; (ii) components with many modes (or short wavelength behavior) are described statistically with SEA, as their dynamic behavior is very sensitive to uncertainty. This partitioning matches the mix of dynamic behavior encountered in the mid-frequency range and also makes the method computationally efficient (since components that would require a large number of deterministic descriptive degrees of freedom are described statistically with SEA).

No information about the nature of the uncertainty in the SEA subsystems needs to be provided as those components are assumed to have a state of maximum uncertainty (for a given modal overlap, damping, and junctions impedance). The hybrid method predicts the mean response across this ensemble and provides a pragmatic nonparametric approach to deal with the lack of information regarding the system uncertainty.

The method has been shown to yield good results for the ensemble averaged response of a number of example systems. The first two validation cases demonstrated how statistics are easily introduced in a standard FE analysis, by modeling modally dense components using SEA subsystems. The third validation case demonstrated how deterministic details can be introduced in a standard SEA model, by modeling with FE the local details of a complex junction between a number of SEA subsystems. The numerical and experimental validations presented in this paper are focused on structure-borne noise problems, so that only point and line junctions have been demonstrated. The hybrid FE-SEA equations are, however, general and apply to any vibro-acoustic system including the coupling of structures and acoustic fluids though area junctions.

ACKNOWLEDGMENTS

The validation part of the work was funded by the Air Force Laboratory, Space Vehicles Directorate, Kirtland AFB, NM, under the SBIR Phase II Contract No. F29601-02-C-0109 managed by Dr. Steven Lane. The testing was performed by Dr. Mike Kidner and Dr. Cory Papenfuss at the Vibration and Acoustic Laboratory of the Virginia Polytechnic Institute.

APPENDIX: LINE IMPEDANCE ALONG THE EDGE OF A SEMI-INFINITE PLATE

Consider a hybrid model where a structural component described with finite elements (FEs) is connected to a plate described with SEA, along a straight junction of finite length L. The direct field dynamic stiffness matrix associated with the boundary degrees of freedom of the plate is found from the analysis of a segment of length L on the edge of the semi-infinite plate.

The displacement field along the segment is described with a set of shape functions: if FE nodal degrees of freedom are used, the shape functions are the elementary shape functions associated with each node in the segment; if a modal decomposition is employed, the shape functions are the mode shapes along the segment. In any case, the displacement at any point is expressed as the sum of the shape function contributions. Assuming thin plate theory, three translations and the rotation of the midplane fully describe the motion of the edge of the plate. Therefore, at any point x along the segment the four displacement components can be written: $[u(x),v(x),w(x),\theta(x)]^{\mathrm{T}}=\Sigma_j q_j \boldsymbol{\varphi}_j(x)$ where $\boldsymbol{\varphi}_j(x)=[u_j(x),v_j(x),w_j(x),\theta_j(x)]^{\mathrm{T}}$ is a shape function with four components.

The ji entry of the direct field dynamic stiffness looking into the plate is written

$$\{D_{\mathrm{dir}}\}_{ji} = \int_{-L/2}^{L/2} \boldsymbol{\varphi}_j^{*T}(x)\mathbf{f}_i(x)dx, \tag{A1}$$

where $\mathbf{f}_i(x)$ is the distribution of the four forces (dual of the four displacements) due to the prescribed displacement field $\boldsymbol{\varphi}_i$ along the segment.

In what follows, the displacement field outside of the junction is assumed to be zero (clamped boundary condition) so that the wave number representation of a given shape function is easily obtained with spatial Fourier transform:

$$\boldsymbol{\Phi}_i(k) = \int_{-\infty}^{\infty} \boldsymbol{\varphi}_i(x)\exp(-ikx)dx. \tag{A2}$$

The integral can be reduced to the interval $[-L/2, L/2]$ due to the clamped boundary condition assumed outside the junction.

The semi-infinite plate wave dynamic stiffness matrix $\mathbf{D}^{\infty}$ relates the four displacement wave number transforms to the four forces wave number transforms $\mathbf{F}_i$ by

$$\mathbf{F}_i(k) = \mathbf{D}^{\infty}(k)\boldsymbol{\Phi}_i(k). \tag{A3}$$

The interest in using the wave number representation is that the matrix $\mathbf{D}^{\infty}$ is analytically expressed in terms of the plate properties.[21] For a thin plate, the bending freedoms w and θ are not coupled to the shear/extension freedoms u and v, and the 4×4 wave dynamic stiffness matrix is thus made of two 2×2 block matrices

$$\mathbf{D}^{\infty} = \begin{bmatrix} \mathbf{D}_{se}^{\infty} & \mathbf{0} \\ \mathbf{0} & \mathbf{D}_{b}^{\infty} \end{bmatrix}. \tag{A4}$$

Applying the inverse Fourier transform to Eq. (A3) yields the force distributions along the edge

$$\mathbf{f}_i(x) = \frac{1}{2\pi}\int_{-\infty}^{\infty} \mathbf{D}^{\infty}(k)\boldsymbol{\Phi}_i(k)\exp(ikx)dk. \tag{A5}$$

Substituting Eq. (A5) into Eq. (A1), and inverting the integration order yields the direct field dynamic stiffness entry as a function of the wave number transforms of the shape functions and the wave dynamic stiffness matrix

$$\{D_{\mathrm{dir}}\}_{ji} = \frac{1}{2\pi}\int_{-\infty}^{\infty} \boldsymbol{\Phi}_j^{*\mathrm{T}}(k)\mathbf{D}^{\infty}(k)\boldsymbol{\Phi}_i(k)dk. \tag{A6}$$

For stress-free boundary conditions outside of the junction, an alternative approach also based on Fourier transform has been developed, which makes use of the semi-infinite plate wave dynamic receptance matrix $\{\mathbf{D}^{\infty}\}^{-1}$.

In the validation case with line junctions presented in the paper, only the bending motion of the panels is modeled with SEA, while the in-plane motion of the panels is modeled with FE. Hence, the direct field dynamic stiffness of the panels only involves the bending contribution $\mathbf{D}_b^{\infty}$ in Eq. (A4) and only concerns the out-of-plane FE degrees of freedoms w and θ along the junction.

[1] M. S. Kompella and B. J. Bernhard, "Measurement of the statistical variation of structural-acoustic characteristics of automotive vehicle," in *Proceedings of the SAE Noise and Vibration Conference*, Warrendale PA (1993).

[2] R. Cornish, "A novel approach to optimizing and stabilizing interior noise quality in vehicles," *Proceedings of the Institute of Mechanical Engineers, Part D* – J. Automobile Eng.**214**(D7), 685–692 (2000).

[3] R. H. Lyon and R. G. DeJong, *Theory and Application of Statistical Energy Analysis* (Butterworth-Heinemann, Boston 1995).

[4] R. S. Langley and V. Cotoni, "Response variance prediction in the statistical energy analysis of built-up systems," J. Acoust. Soc. Am. **115**(2), 706–718 (2004).

[5] A. K. Belyaev and V. A. Palmov, "Integral theories of random vibration of complex structures," in *Random Vibrations – Status and Recent Developments*, edited by I. Elishakoff and R. H. Lyon (Elsevier, Amsterdam, 1986).

[6] C. Soize, "A model and numerical method in the medium frequency range for vibroacoustic predictions using the theory of structural fuzzy," J. Acoust. Soc. Am. **94**(2), 849–865 (1993).

[7] R. S. Langley and P. Bremner, "A hybrid method for the vibration analysis of complex structural-acoustic systems," J. Acoust. Soc. Am. **105**(3), 1657–1671 (1999).

[8] V. Jayachandran and M. W. Bonilha "A hybrid SEA/modal technique for modeling structural-acoustic interior noise in rotorcraft," J. Acoust. Soc. Am. **113**(3), 1448–1454 (2003).

[9] R. M. Grice and R. J. Pinnington, "Analysis of the flexural vibration of a thin-plate box using a combination of finite element analysis and analytical impedances," J. Sound Vib. **249**(3), 499–527 (2002).

[10] L. Ji, B. R. Mace, and R. J. Pinnington, "A mode-based approach for the mid-frequency vibration analysis of coupled long- and short-wavelength structures," J. Sound Vib. **289**(1-2), 148–170 (2006).

[11] S. B. Hong, A. Wang, and N. Vlahopoulos, "A hybrid finite element formulation for a beam-plate system," J. Sound Vib. **298**(1-2), 233–256 (2006).

[12] P. J. Shorter and R. S. Langley, "Vibro-acoustic analysis of complex systems," J. Sound Vib. **288**(3), 669–699 (2005).

[13] P. J. Shorter and R. S. Langley, "On the reciprocity relationship between direct field radiation and diffuse reverberant loading," J. Acoust. Soc. Am. **117**(1), 85–95 (2005).

[14] R. S. Langley, "On the diffuse field reciprocity relationship and vibrational energy variance in a random subsystem at high frequencies," J. Acoust. Soc. Am. **121**(2), 913–921 (2007).

[15] R. S. Langley and V. Cotoni, "Prediction of the ensemble mean and variance of the response of uncertain structures using the Hybrid FE-SEA method," in *Proceedings of ISMA2006 Conference*, Leuven, Belgium, September 18–20 (2006).

[16] R. S. Langley and P. J. Shorter, "The wave transmission coefficients and coupling loss factors of point connected structures," J. Acoust. Soc. Am. **113**(4), 1947–1964 (2003).

[17] R. S. Langley, P. J. Shorter, R. H. Lande, and V. Cotoni, "Hybrid deterministic-statistical modeling of built-up structures," in *Proceedings of ICSV12 Conference*, Lisbon, Portugal, July 11–14 (2005).

[18] R. S. Langley, "Natural frequency statistics and universality," in *Proceedings of ICSV12 Conference*, Lisbon, Portugal, July 11–14 (2005).

[19] VA ONE 2006 User's Guide, The ESI Group Oct. 2006.

[20] B. R. Mace and P. J. Shorter, "Energy flow models from finite element analysis," J. Sound Vib. **233**(3), 369–389 (2000).

[21] R. S. Langley and K. H. Heron, "Elastic wave transmission through plate/beam junctions," J. Sound Vib. **143**(2), 241–253 (1990)